Propagated Ridge Structure and Faulting as a Control on Sediment Accumulation

Casey K Hearn

University of Washington
1501 NE Boat Street
Marine Sciences Bldg, Room 255
Seattle, WA 98105

ckh3@u.washington.edu

June 1st, 2012

Non-Technical Summary

In the Eastern Tropical North Pacific within the Sea of Cortez lies a unique geologic feature. Three tectonic plates spread and twist apart over millions of years as brand new sea floor is created, leaving a wide range of unique topographies. Three thousand meters above, in the surface ocean, a rain of biological waste products sinks slowly down to blanket the sea floor in a thickening layer of organic ooze. In March of 2012, I embarked on a research cruise aboard the *Thomas G. Thompson* to study the effect of seafloor topography on the distribution of sediment in this area by using sonar imaging. The high resolution multibeam sonar on the Thompson enabled me to construct datasets containing topography and sediment significance across the area. By comparing these data through a series of measurements describing different aspects of the topography, I was able to establish relationships between geologic features and the pattern of sediment. My results show that three unique zones of sediment distribution topographic control exist in this one study area. In the first zone near the spreading center, small ridges loosely guide some sediment into troughs while it accumulates over the entire region like a blanket of snow. In the second zone, large scale ridge systems shed sediment off steep slopes to be concentrated in ponds at the bottom of troughs. The third zone is affected by the pulling forces of diverging plates, causing long faults to break the thick sediment blanket into flat plateaus and valleys. This research concludes that tectonic, physical ocean, and biological process are uniquely linked in a variety of ways to control the distribution of sediment in this fascinating portion of the seafloor.

Acknowledgements

I would like to thank all instructors for the Oceanography Senior Field course for their extraordinary effort in managing and guiding so many independent projects simultaneously while still finding time to mentor students individually. The marine geology and geophysics course advisor Miles G. Logsdon was exceptionally helpful in cultivating this project from idea inception through the final stages of manuscript composition. My fellow students were among my greatest supporters throughout this endeavor, with special advice given by George Roth, Kira Homola and Catherine Wardell. I would also like to thank the crew of the Thomas G. Thompson for their dedication to student learning and inestimable patience throughout the instruction of shipboard activities. I would also thank Mark Holmes, Jim Postel and Justin Smith for their commendable extra effort in cruise preparation. Finally, I would like to sincerely thank my mentor, Professor H. Paul Johnson, for his wise counsel and numerous contacts that helped ensure this project's success.

Abstract

The pattern of sediment accumulation (distribution and thickness above basement rock) across the seafloor of the Pacific/Rivera/North American plate triple junction is controlled by sub-mesoscale topographic roughness of the basement rock. On board the R/V *Thomas G. Thompson* in March of 2012, a Kongsberg EM302 multibeam swath bathymetry echosounder was used to survey several transects crossing ridge propagations from a traditional spreading center, a non-transform offset, and a slip-strike fracture zone. In post processing, rugosity metrics (measure of small scale variations in surface height) of the refined multibeam data surface (CUBE at ≈20m resolution) were applied over focused study sites containing distinct seafloor ridge structures to assess influences of local topography. Derived outputs from these metrics were combined with measured backscatter intensity and compared with a series of profiles describing topographic slope. Comparison of these profiles enabled a comprehensive analysis of the effect of basement rugosity on sediment accumulation throughout the region. The spatial distribution of sediment is interpreted as 3 separate bottom type regimes uniquely linked to physical processes. Sediment accumulation patterns on basement rock close to the spreading axis is controlled by small scale high frequency ridge systems while sediment draping is only slightly non-uniform. At greater distances from the spreading center, lower frequency high-magnitude ridge sets control downslope gravity driven sediment transport to cause ponding in troughs. Within the Rivera Fracture Zone, tectonic tensional forces create slip strike fault scarps at high slopes that are free of sediment. At this extraordinary study site, structural expressions of tectonic processes interact with physical ocean currents and the biological carbon pump to influence morphology of sediment accumulation: a stunning interplay of constituents. Research on scale effects of seafloor topography at this site can help explain patterns of sediment accumulation at ridge systems throughout the world's oceans.

Introduction

Beginning with the fragmentation of the Farallon plate (≈28 mya), many small oceanic plates were isolated, deformed and subducted beneath the North American Continental Plate or sutured to the Pacific Plate (C. DeMets and S. Traylen, 2000)(Fig. 1). Unique amongst these was the Rivera Plate, which has survived through to the present due to nearly matching rates of spreading on its western boundary and subduction under Mexico on the eastern flank. A slow net-rate of subduction is occurring as shear forces from the adjacent spreading center of the Pacific and Cocos Plates deform and rotate the much smaller Rivera Plate (C. Demets and S.

Sten, 1990). As one of only two locations of the junction between three ocean plates in the Pacific Ocean, the northern tip of the Rivera Plate is a unique tectonic interface for the study of the effect of propagated seafloor ridge frequency, magnitude and morphology on the pattern of sediment accumulation.

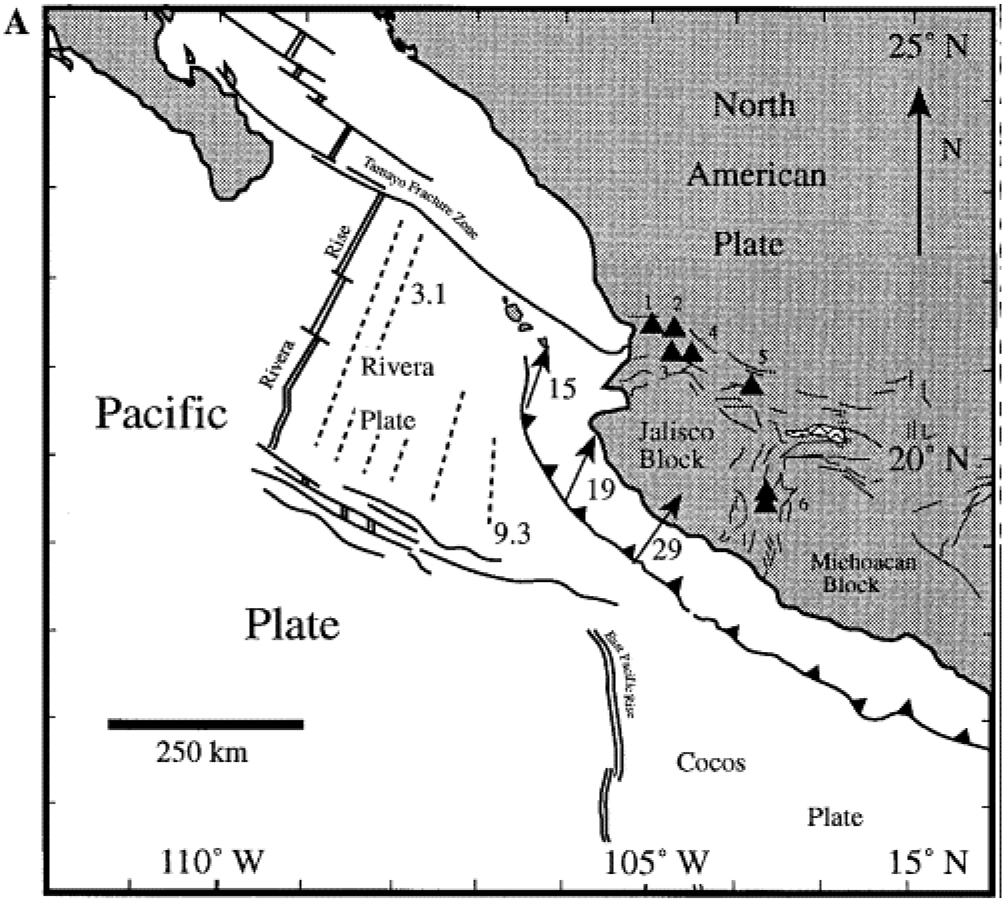

Fig. 1. Tectonic map of the Rivera Plate. Magnetic anomaly isochrons shown in millions of years. Along the eastern boundary, net subduction rates are shown in millimeters per year: note the north-south trend in subduction, attesting to the ongoing rotation of the Rivera Plate. Figure and caption adapted from (Nichol et al. 2011).

Across the spatial extent of a relatively small (46 by 32km) study area focusing on the triple junction, there will be negligible variability in average annual rates of surface primary production (Hauschild et al, 2003). Patchiness in surface production occurs regularly across most oceans, but becomes irrelevant for sedimentation rates across small areas when integrated over long time scales (Hauschild et al, 2003). For an ideal region with a flat seafloor, this would suggest uniform a rate of pelagic sediment deposition in the form of calcareous ooze. With no known hydrothermal vents along the Rivera/Pacific or Rivera/Cocos ridges, the rate of benthic organic carbon production should also be held constant throughout the study site, precluding any spatial bias in sediment accumulation rates due to benthic biological production or consumption. Furthermore, the maximum depth water depth within the study area was no more than 3350m, well above the carbonate compensation depth (CCD). At depths greater than the CCD, active dissolution of calcium-carbonate structures occurs and greatly influences the depth and composition of marine sediment. Assuming this uniform sedimentation rate with respect to both time and space, the sediment thickness within the Rivera Triple-junction study area should increase uniformly with crustal age. Given the fast spreading rate (>20mm/yr) of the East Pacific Rise, little variation in spreading rate should occur through time, thus sediment thickness should also increase linearly with distance from the spreading ridge axis (C. Demets and S. Sten, 1990).

Hydrothermal vent systems on ridge axes emit plumes of reduced chemical compounds that feed a highly productive microbial ecosystem. The subsequent production of particulate organic carbon in such systems can greatly enhance levels of abyssal and mid-water biogenic deposition across the local down-current portion of the seafloor (Hauschild et al, 2003). In the aforementioned study, the hydrothermal plumes were the predominant factor in constraining sediment depth, rather than bathymetry. In the proposed study area for this project, no hydrothermal vents have been identified, and thus seafloor structure (rugosity and ridge orientation) should be the principle control on sediment accumulation, allowing the effects to be empirically quantified.

In an environment of uniform sedimentation rates, the dominant control on distribution becomes the physical structure of the bedrock. A recent study concluded that ridge wall morphology and the leeward or currentward ridge line orientation (that is, if current is predominately across or along the ridge axis, respectively) have a direct impact on sediment draping (Lastras et al. 2011). Any variability in observed sediment thickness can therefore be attributed to physical processes, such as downslope gravity transport or bottom boundary transport by abyssal currents (controlled by seafloor rugosity and ridge orientation). Seafloor roughness is the predominant control on rates of abyssal diapycnal mixing (mixing across isopycnals) through interactions with tidal currents that produce turbulent eddies (Decloedt and Luther 2010). In most abyssal environments the greatest magnitude currents are produced by diurnal and semi-diurnal tides which flow in opposing directions along the same axis. Seafloor ridge structures that share the orientation of this axis (currentward) will generate less turbulence than similar structures at perpendicular angles (leeward) (Nichol et al. 2011).

High resolution swath bathymetry data was recently used to analyze the morphological expression of major fault systems off the coast of Baja California (Fig. 1; Michaud et al. 2004); a direct analog application of studying geomorphic processes through the interpretation of bathymetric data. The fine mapping scales available through the use of high resolution swath bathymetry has enabled quantitative analysis of physical and geologic oceanographic processes by allowing scientists to identify the spatial extent of geomorphic features (Nichol et al. 2011), making calculations of slope possible even for small scale features.

Following the aforementioned previous research, I hypothesized that in the area of the Rivera Plate Triple-junction, ridge sets with lower topographic magnitude (vertical depth range from ridge crest to trough bottom), greater spacing (lower frequency) and lower flank rugosity at an orientation parallel to the axis of tidal currents will trap more pelagic sediment and thus increase rates of sediment accumulation. I also expected to see areas of greater sediment ponding in troughs between ridges displaying the aforementioned characteristics. I anticipated that significant ridge crests should provide an impediment to abyssal tidal currents, increasing turbulence over crests (reducing sediment thickness) while reducing bottom boundary shear on ridge flanks and in troughs, allowing some sediment to settle. I sought to explore the relationship between ridge frequency and basement rock rugosity, predicting that higher frequency sets would have greater magnitude variability in height over the same distance. Within the study area, I expected to see ridge principle ridge orientation vary by as much as 30 degrees due to the presence of non-transform offsets (as can be estimated from previous low resolution bathymetry of the study area). I sought to determine whether high frequency ridge sets with greater rugosity and leeward orientation would increase rates of diapycnal mixing to reduce settling velocities of sinking particles, thus reducing sediment accumulation. In all ridge environments, these processes should have produced a noticeable absence of sediment on steep ridge flanks and crests while increasing accumulation in troughs.

In a unique setting such as the Rivera triple junction, several major contributing factors to sediment accumulation patterns may be held constant or deemed trivial, enabling the influence of ridge rugosity and orientation to be studied directly. Very few sites afford scientists the ability to study interactions between biological primary production, physical ocean currents, tectonic structures and geomorphology. This investigation can improve our understanding of the relationship between ridge orientation, roughness and sediment accumulation patterns over a highly tectonically active and complex area of seafloor. Extrapolating the results of this study will help researchers tackle questions of scale pertaining to seafloor topography at ridge systems throughout the world. Indirectly, the distribution of benthic organisms, which rely on mineralization of surface-produced organic matter, may be better modeled at ridge systems by expanding the results of this study. Additionally, the composition of sediment ponds in subducted oceanic plates may be better constrained by understanding accumulation patterns and deposition rates, with direct consequences for fore-arc vulcanology. Many avenues of continued research could help apply the results of this project by applied to the biological and volcanic realms of ocean sciences.

Methods

A bathymetric survey of the Rivera Plate Trip-junction was conducted on board the *Thomas G. Thompson* on 18 March, 2012 using a Kongsberg EM302 Mutibeam Echosounder (Fig. 2). Average survey line spacing was 7.2km using a 60 degree beam angle to maximze coverage while preventing data holes (≈10% overlap). Survey time was 16.5hrs while maintaining a speed of ≤6 knots during which sea state conditions did not rise above 2. Sound velocity profiles were obtained from CTD casts at the beginning and middle of the survey, and from expendable bathythermograph (XBT) deployments at the first and third quarter marks. SVP profiles were uploaded to the acquisition software shortly after being acquired.

Post processing of bathymetric data was performed using CARIS HIPS and SIPS ver. 7.1. Spatial variability from temperature and salinity trends with depth in local CTD casts was minimal, thus SVP profiles for individual lines were chosen on a basis of temporal proximity. Tidal variation during the survey was minimal due the proximity to the regional M2 amphidromic point; thus given the water depth and necessary survey precision, a zero tide file was chosen for all lines. A 20m CUBE (Combined Uncertainty Bathymetric Estimator) surface was created from the survey lines using default vessel instrument uncertainty values for the R/V

Thomas G. Thompson. Extensive surface cleaning (a process taking ≈10 hours) removed erroneous data and spikes with special care taken in areas of rough topography to preserve all small to moderate scale features.

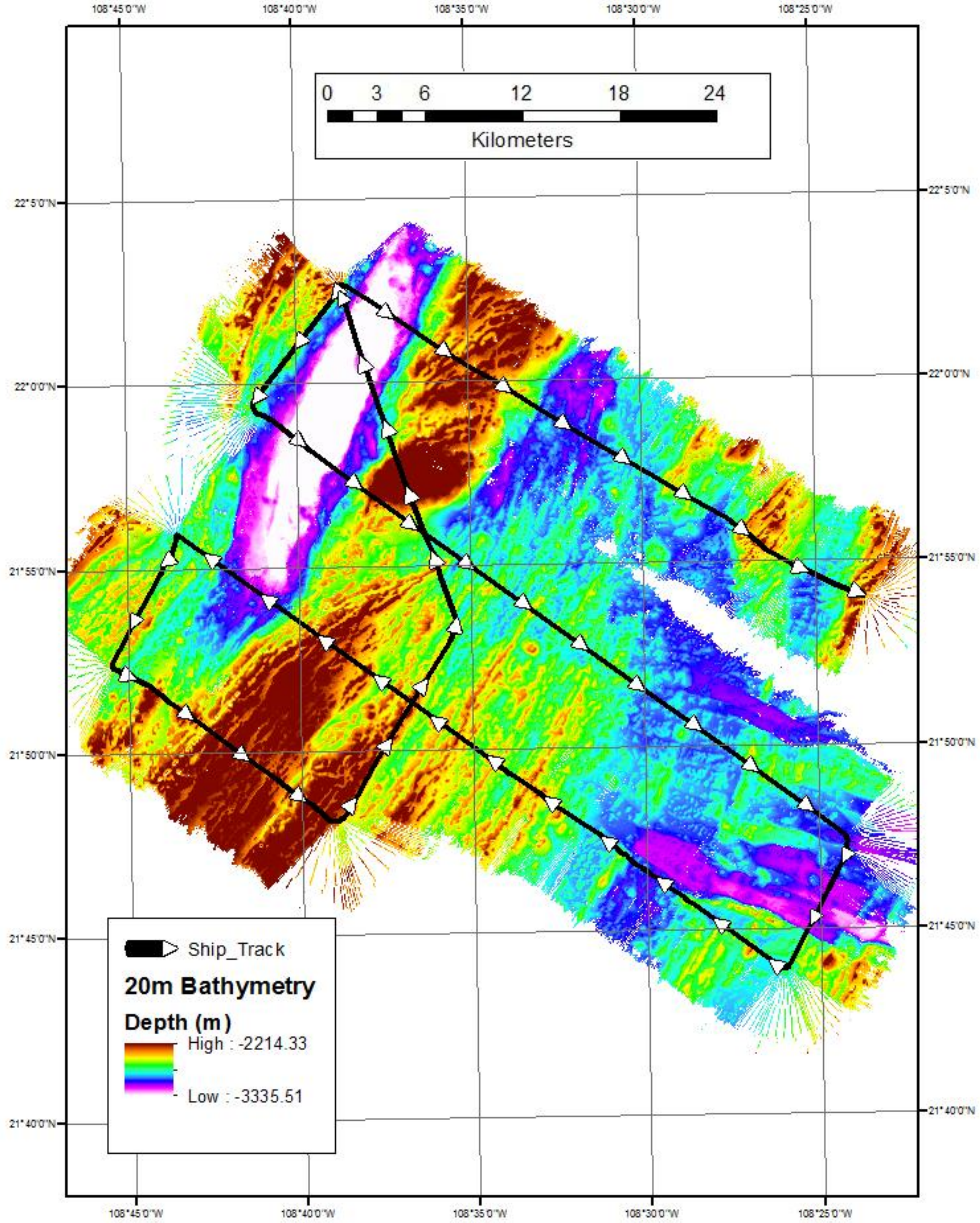

Figure 2. Bathymetric map of the Rivera Plate Triple-Junction from EM 302 multibeam echosounder. Final surface created by CUBE function at 20m resolution. Cleaned to remove false returns and errors.

The GeoCoder toolset within CARIS HIPS and SIPS was used to create GeoBar files for each survey line. These files were mosaicked together using a line proximity blending technique to create a single dataset of the intensity of signal backscatter return. These steps created two separate georegistered raster datasets, one containing only depth information while the other dealt with intensity of backscatter return. It is in the contextual framework of the depth dataset that intensity of return information was used to infer spatial variation in sediment distribution.

After the conclusion of cleaning, the bathymetric surface and intensity dataset were exported to ArcGIS for spatial analysis. A zonal slope function (maximum slope from change in Z between focus cell and all adjacent cells) was performed on the topographic surface to create a slope raster. Topographic rugosity was determined using the Jenness enterprises (J. Jenness 2012) surface area and ratio toolset for the bathymetric surface. This zonal function creates a representative triangular matrix surface for each raster cell with radial facets of area proportional to the variation in Z between that cell and the neighboring cell in the direction of the facet (Fig. 3). A ratio of the total surface area for the triangular surface of that cell to the area of a flat surface of equal dimensions is used as the standard metric for topographic roughness.

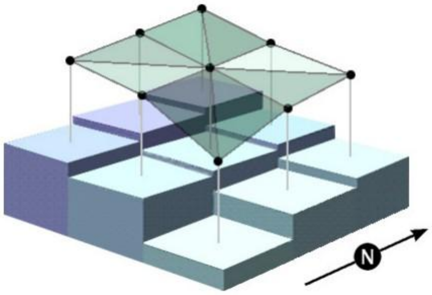

Figure 3. Visual representation of Jenness Enterprises surface area function. Adapted from toolset user maunaul, 2012.

Within the full extent of the survey area, specific focused study sites were chosen based on certain criteria with the intent of covering the full range of topographic features and bottom types (Fig 4). Study sites of comparable areas were placed within bands at moderate distance from track lines due to the reduction in data quality for intensity of backscatter return from angles both close to and far from nadir (at distances <1 and >3km from ship track lines). For each individual study site, the roughnesses of all included cells were averaged to generate a single topographic roughness value.

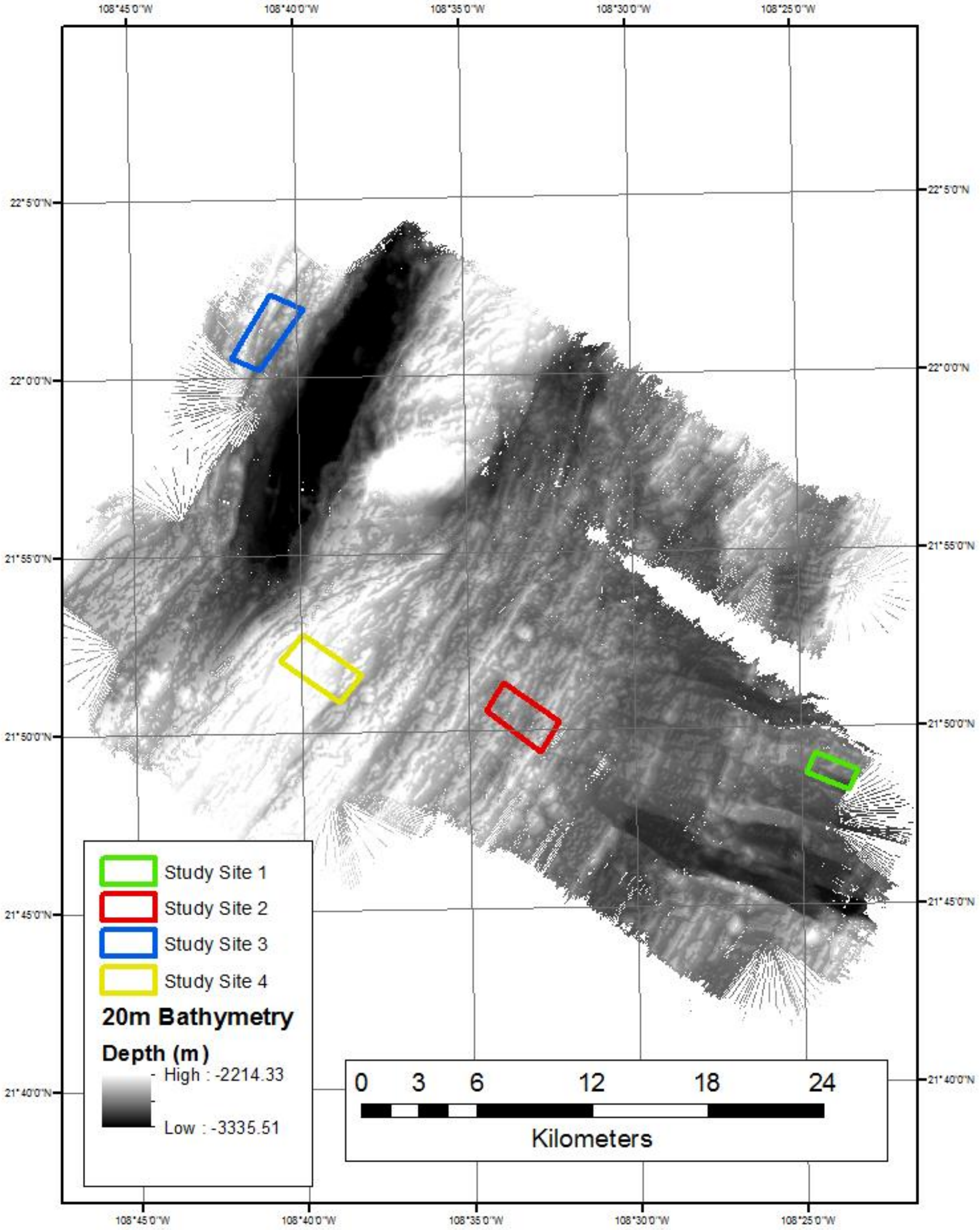

Figure 4. Locations of focused study sites within the greater study area.

A classification algorithm function was run on the topographic surface for 3 classes at natural breaks to isolate and quantify regions of high, low and moderate slope. Similarly, a 5 class natural break classification function was performed on the intensity dataset to isolate areas of very low, low, moderate, high and very high intensity of backscatter return (Fig. 7). The ArcGIS profile tool (3D analyst toolset) was used to create profiles for elevation, intensity and slope along the long axis of each study area. Data was exported from each profile for analysis and display in Microsoft EXCEL 2007. Additional surface functions were run on the bathymetry surface to create datasets for topographic position index, flow direction, flow accumulation and flow length for visual comparison purposes.

Commonly Used Terms

Study Area: Full extent of the bathymetric survey encompassing the Rivera Triple Junction.

Study Site: Specific region of intensive analysis within the greater study area upon which zonal functions were performed (four sites total).

Regime: Region of seafloor wherein the distribution of sediment is primarily controlled by a unique tectonic or physical process.

Results

Analysis of intensity of return class vs slope class revealed variable levels of coupling between study sites (Fig. 5). In site 1 (n=5384), areas of very high intensity of return contained the highest portion of high slope areas (42%), while the area of very low intensity of return contained mostly low slope cells (95%). A negative trend existed between percentage of low slope cells contained and intensity of return. Conversely, percentage of high slope areas increased with higher intensity of return. Topographic roughness at this site was the lowest at 1.031. At site 2 (n=7919) there were no cells of very low intensity of return and there were no statistically significant trends with increasing intensity. Here, topographic roughness was 1.072. Site 3 (n=6404) showed muted versions of the intensity trends obvious at site 1, with significant coupling between high slope areas and increasing intensity of return. Only 12 cells within this site had very low intensity values. Topographic roughness for site 3 was the highest found, at 1.133. At site 4 (n=6482) there were no trends in low or medium slope, but a strong increase in the percentage of high slope areas (n=2333) contained within very high intensity cells. At this site, topographic roughness was again high at 1.111. Topographic roughness varied from 1.031 in site 1 to 1.133 in site 3 (difference of .102).

Profiles of intensity of return and topographic slope also displayed varying degrees of agreement, depending on study site (Fig. 6). Signal to noise ratio for intensity of return was markedly higher than depth for all study sites, but varied by area (maximum in peripheral portions of full survey area, minimum near ridge axis and along ship track nadir). At site 1, ridge frequency was moderate while coupling between intensity and slope peaks was close; signal to noise ratio for intensity was high.

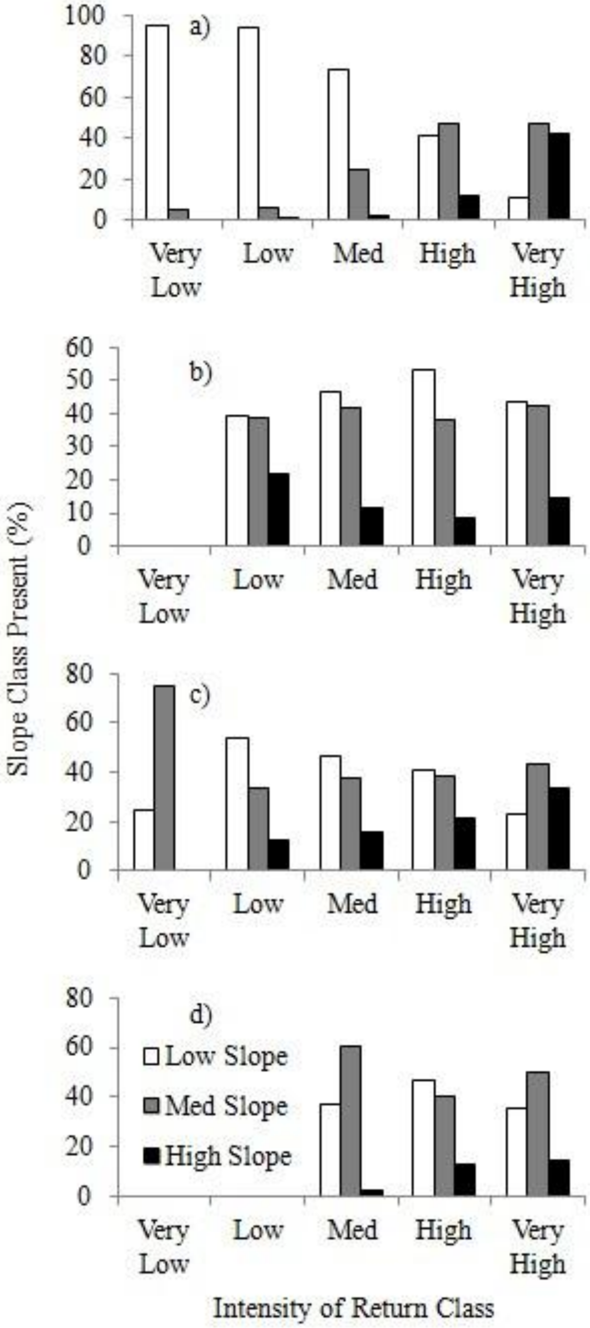

Figure 5. The percentage of each slope class present in cells of varying intensity of return class. Each panel contains results from an individual study site, listed 1-4 (a-d respectively).

Site 2 had the highest frequency of ridges and no statistically significant coupling with slope; signal to noise ratio for intensity was very low. Site 3 had the lowest frequency of ridges and a moderately close coupling between intensity and slope; signal to noise ratio was moderate.

Topographic depths within the full study area ranged from 2214m at the northern offset peak to 3335m in the northern axial depression (full range of 1121m) with a very general decreasing trend in elevation with increasing distance from the spreading ridge on the eastern side. Intensity of backscatter return varied from -0.015 to -47.37, with both the highest and lowest values found directly along the ship track line.

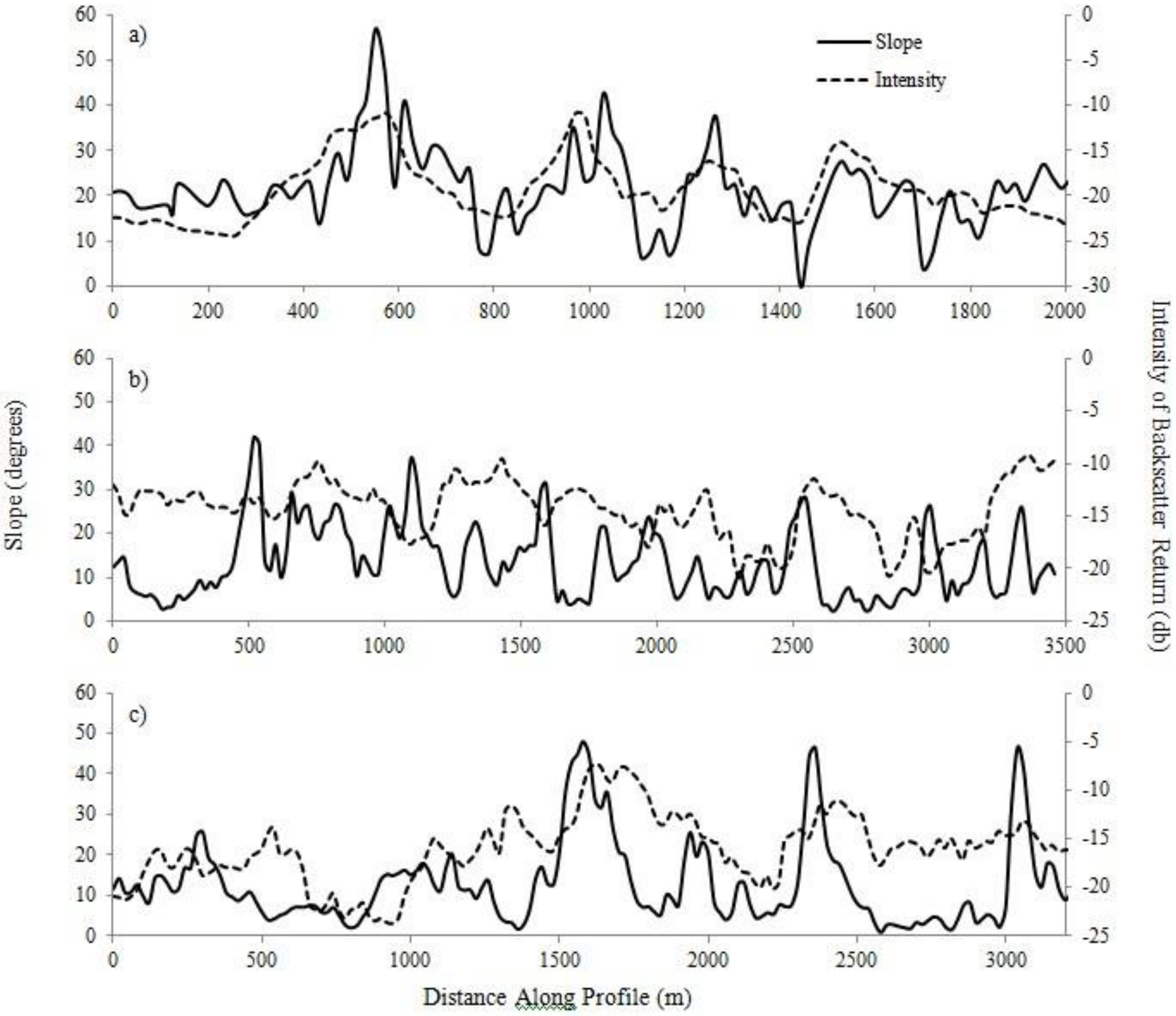

Figure 6. Profiles of slope and intensity of return against distance along the profile. Panels correspond to profiles from individual study sites, ordering 1-3 (a-c respectively).

Figure 7. Distribution of intensity classes throughout the Rivera Plate Triple-junction. Class distribution is shown graphically with color choices made to visually represent intensity groups.

Discussion

The evidence presented here describes a complex bathymetric system where the distribution of sediment is controlled by several key parameters. Within the full study area, several regimes of distinctive morphological features have emerged (Fig. 8). In each regime, topographic roughness, ridge height and frequency, influence of the fracture zone, and distance from the spreading ridge contribute to the pattern of sediment distribution. The tectonic history of the region has likely played a significant role in controlling the geomorphic form of the seabed (Nichol et al. 2011). Due to the limited resolution and quality of intensity data recovered and the restricted size of the full survey area, the effect of ridge orientation on sediment distribution due to interaction with tidal currents was difficult to confidently describe. However, this observation carries an important suggestion: abyssal tidal currents in the area may be of a sufficiently low magnitude to have little impact on the distribution of sediment in the ridge zone. Regardless of the underlying process, the impact of tidal currents can be assumed a far less significant contributor to sediment distribution than topographic features.

The strongly bimodal distribution of intensity values across the entire survey area suggests two dominant bottom types. The high intensity value peak suggests a solid surface composition capable of strong signal reflectance. In previous studies extensive ROV photographic ground-truthing of return intensity values has demonstrated the relationship between well consolidated hard surfaces with strong signal returns (Lastras et al. 2011). Representative cells from the higher classes appear most commonly near the axis of spreading; the geologic nature of spreading ridges suggests that this bottom type is composed primary of uncovered or lightly covered porous basalt. The low intensity peak conversely corresponds to a soft surface more likely to absorb an incoming high frequency signal. Once again, observing that the distribution of these low intensity areas dominates the flat topography farther from the spreading ridge, it is suggested that these are moderate to heavily sedimented bottoms. There is a transition region between the two dominant endmembers comprised of basalt with an intermediate covering of sediment.

The site specific intensity vs slope metrics indicate significant spatial trends in sediment distribution and its constituents. In areas with low topographic roughness far from the spreading ridge axis, sedimentation is thick and only high slope features show exposed bedrock (evident in strong return intensities). As topographic roughness decreases, sediment cover becomes more complete and its distribution dependence on smaller scale topography becomes reduced. In areas close to the ridge axis, smaller scale ridge features control sediment distribution, however the low signal to noise ratio and coarse resolution of bathymetric data make these features difficult to resolve. The site profiles suggest a strong coupling between sediment ponding and ridge magnitude. Low magnitude ridge systems have a small topographic range and high frequency, while high magnitude systems have large ranges from trough to crest and long distances between successive crests. In the former system, sediment pattern is controlled by topography temporarily with decreasing significance as crustal age increases. In contrast, high magnitude systems enhance gravitational sediment transport downslope with significant ponding occurring in troughs and continue to dominate accumulation patterns at much greater distances/ages from the axis of spreading. Gravitational transport due to significant topographic features is thus the key process controlling sediment distribution.

Direct comparisons between ridges of varying orientations were difficult given that no two ridge patches were sufficiently similar. Despite morphological similarities between ridge groups differences in age, distance from spreading center, and surrounding topography reduced confidence in results. A more comprehensive survey may capture similar ridge structures of varying orientation so that a more controlled comparison could be attempted. Curiously, on the edges of the survey, several high ridge set features were observed. These features may indicate an inconsistent magma supply to the spreading axis. Ancient periods of high magma supply may correspond to these high elevation ridge sets. Large low regions between subsequent highs may correspond to periods of lower magma supply when detachment faulting from tectonic tensional forces stretched the new plate material and caused characteristic high magnitude ridge-trough features.

Across the eastern portion of the study area, several-kilometer long perpendicular high slope features are evident. The proximity to the Rivera Fracture Zone suggests that these are surficial extents of slip-strike and detachment faults. Expressions of slip-strike faults are typically much less conspicuous, shorter lived and less continuous than those near convergent boundaries (Michaud et al. 2004). However, within the Rivera Triple Junction, the crust is sufficiently young for sediment coverage to be thin, allowing small scale tectonic features to be evident. Significant tectonic torque is generated by the motions of all three plates and surface distortions are to be expected. As newly formed basalt moves away from the ridge axis, it cools through conduction and hydrothermally assisted convection and becomes more brittle while experiencing this enhanced torque. A tipping point is reached some 10km from the spreading center and slip-strike faults appear in the sediment distribution. In areas of low topographic roughness at distances greater than 10km from the spreading axis, tectonic deformation within the fracture zone becomes the dominant control on sedimentation by removing accumulated sediment from fault scarps and concentrating material within local basins and troughs. This process created a landscape of tiered plateaus separated by sharp faults

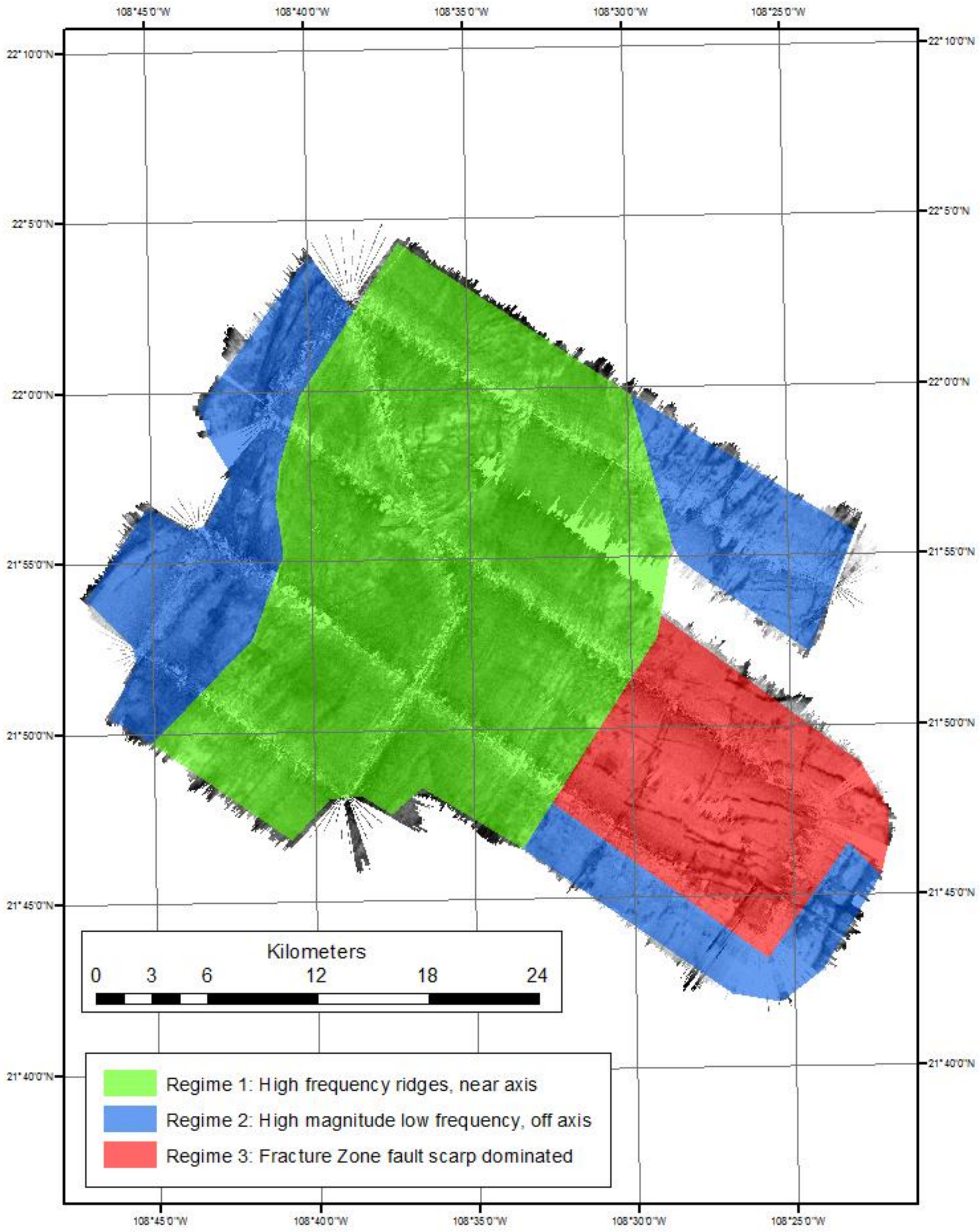

Figure 8. Spatial extent of sediment distribution control regimes within the Rivera Triple Junction.

Conclusions

This investigation provides strong evidence for small scale topographic feature control on sediment distribution within the study area of the River Plate Triple-Junction. Three regimes of unique morphology indicate separate process dominating sedimentation patterns. Near the axis, small magnitude high frequency ridge sets focus some sediment into troughs, while a light blanket builds up over the entire area. Far from the spreading ridge, only high magnitude low frequency structures remain exposed and downslope gravity driven transport moves sediment from ridge crests and flanks into troughs where ponding occurs. Within the Rivera Fracture Zone, tectonic tensional forces cause slip-strike and detachment fault scarps that shed sediment resulting in tiered sedimented plateaus divided by steep faults. This research has only just scratched the surface of sediment analysis for abyssal systems and many important questions still remain to be answered. A survey on greater spatial scales would encompass additional features including more high magnitude ridge sets, additional fault scarps and seamounts. Since sedimentation rates within troughs are higher than on ridge crests, the rates of oxygenic microbial degredation of organic matter may be impacted, resulting in altered chemical composition from sediment that falls evenly and slowly. Subducting plates that entrain sediment will take more material from these fast accumulating ponds due to their low topography. Additionally, the added fault scarps created by the Rivera Fracture Zone expose more bedrock to the seawater, enhancing rates of cooling by hydrothermal circulation. Future research could examine the effect of this forcing on the heat budget of new Rivera Plate rock. For an additional study of high importance for this area, I would propose a series of conductive heat flow profiles across the Rivera Plate covering sedimented areas both within and outside the fracture zone. The results of that study could vastly contribute to our understanding of crustal cooling and help constrain the location of the megathrust fault “locked zone” at the axis of continental convergence.

This study has demonstrated the connection between biological, physical ocean, and tectonic process in a complex region of seafloor. These conclusions could be extrapolated to other regions with similar features, enabling better modeling of sediment distribution and oceanic plate heat budgets throughout the world’s oceans.

References

DeMets, C., and S. Stein. 1990. Present-day Kinematics of the Rivera Plate and Implications for Tectonics in Southwestern Mexico. J. Geophys. Res. **95:** 21,931-21,948, doi:0148-0227/90/90JB-01836$05.00.

DeMets, C. and S. Traylen. 200. Motion of the Rivera plate since 10 Ma relative to the Pacific and North American plates and the mantle. Tectonophysics. **318**: 119-159.

Friedrich, T., A. Timmermann, T. Decloedt, D. S. Luther, and A. Mouchet. 2011. The effect of topography-enhanced diapycnal mixing on ocean and atmospheric circulation and marine biogeochemistry. Ocean Modelling **39**: 262-274.

Hauschild, J., I. Grevemeyer, N. Kaul, and H. Villinger. 2003. Asymmetric sedimentation on young ocean floor at the East Pacific Rise, 15 degrees S. Marine Geology **193:** 49-59.

Jenness, J. 2012. DEM Surface Tools. Jenness Enterprises. Available at: http://www.jennessent.com/arcgis/surface_area.htm.

Lastras, G. et al. 2011. Understanding sediment dynamics of two large submarine valleys from seafloor data: Blanes and La Fonera canyons, northwestern Mediterranean Sea. Mar. Geo. **280**: 1-4,20-39, doi: 10.1016/j.margeo.2010.11.005.

Michaud, F. et al. 2004. Motion partitioning between the Pacific plate, Baja California and the North American plate: The Tosco-Abreojos fault revisited. Geophys. Res. Lett. **31,** doi:10.1029/2004GL019665.

Muller, C. J., and O. Buhler. 2009. Saturation of the Internal Tides and Induced Mixing in the Abyssal Ocean. J. Phys. Ocean. **39**: 2077-2096, doi: 10.1175/2009JPO4141.1.

Nichol, S., A. Heap, and J. Daniell 2011. High resolution geomorphic map of a submerged marginal platea, northern Lord Howe Rise, east Australian margin. Deep-Sea. Res. Pt II. **58**: 889-898.

Van Walree, P. A., J. Tegowski, C. Laban, and D. G. Simons. 2005. Acoustic seafloor discrimination with echo shape parameters: A comparison with the ground truth. Continental Shelf Research **25:** 2273-2293.